





Article

Calibration of Methods to Estimate Solar Irradiance in Northeastern Pará

João Vitor de Nóvoa Pinto¹ , Hildo Giuseppe Garcia Caldas Nunes²,
Daniely Florencia Silva de Souza² , Deborah Luciany Pires Costa¹ ,
Paulo Jorge de Oliveira Ponte de Souza^{1,2} 

¹*Progama de Pós-Graduação em Agronomia, Universidade Federal Rural da Amazônia, Belém, PA, Brazil.*

²*Instituto Socioambiental e dos Recursos Hídricos, Universidade Federal Rural da Amazônia, Belém, PA, Brazil.*

Received: 23 December 2019 - Accepted: 26 December 2019

Abstract

Two models aimed to estimate solar irradiance were calibrated in six locations in Northeastern Pará (Belém, Cametá, Conceição do Araguaia, Marabá, Soure, and Tucuruí). The first one is the equation of Angström-Preseott (AP), which requires observations of sunshine duration hours. The second model is a modified version of Hargreaves' radiation formula (MH), which requires observations of daily maximum and daily minimum air temperatures. Both models were calibrated to estimate daily and monthly solar radiation. The calibration of both equations for each season (i.e., dry season and wet season) in each location was also tested. AP has an average performance about 74% higher than MH for daily estimates (excluding Soure) and 83% higher than MH for monthly estimates (excluding Soure and Tucuruí). The use of seasonally calibrated equations slightly improves the performance of AP, measured by the performance index, by 0.68% and improves the performance of MH in most locations, when estimating daily solar radiation. The performance of both models is much higher when estimating monthly solar radiation than daily solar radiation, with an increase of the performance index of 10.95% for AP.

Keywords: global radiation, evapotranspiration, Angström-Preseott, temperature, sunshine duration hours.

Calibração de Métodos para Estimativa da Irradiância Solar no Nordeste do Pará

Resumo

Dois modelos destinados a estimar a radiação solar incidente na superfície terrestre foram calibrados em seis localidades no nordeste do Pará (Belém, Cametá, Conceição do Araguaia, Marabá, Soure e Tucuruí). O primeiro é a equação de Angström-Preseott (AP), que requer observações do número de horas de brilho solar. O segundo modelo é uma versão modificada da fórmula de radiação de Hargreaves (MH), que requer observações da temperatura máxima e mínima diárias. Ambos os modelos foram calibrados para estimar a radiação solar diária e mensal. A calibração de ambas as equações para cada estação (i.e., estação menos chuvosa e estação chuvosa) em cada localidade foi também realizada. AP tem desempenho cerca de 74% maior que MH para estimativas diárias (excluindo Soure) e 83% para estimativas mensais (excluindo Soure e Tucuruí). O uso de equações calibradas para cada estação aumenta em 0,68% o desempenho de AP e também aumenta o desempenho de MH, medido pelo índice de desempenho, na maior parte das localidades, nas estimativas de radiação solar diária. O desempenho de ambos os modelos é muito maior quando estimando a radiação solar mensal em relação a radiação solar diária, com aumento do índice de desempenho de, em média, 10,95% para AP.

Palavras-chave: radiação global, evapotranspiração, Angström-Preseott, temperatura, horas de brilho solar.

1. Introduction

Global horizontal irradiance has a linear relationship with sunshine duration hours, which is described by the Angström-Prescott equation (AP). However, its intercept (a_s) and slope (b_s) must be calibrated so it can provide reliable estimates (Allen *et al.*, 1998). The calibration is performed by linear regression and requires simultaneous measurements of both global horizontal irradiance and sunshine duration hours. Moreover, Allen *et al.* (1998) recommend Hargreaves' radiation formula to estimate the fraction of solar extraterrestrial radiation that reaches Earth's surface when measurements of sunshine hours are not available. This formula may be useful, since it requires only the difference between daily maximum and minimum air temperature, both of which are widely available data, but Hargreaves' formula also requires calibration.

When calibrated coefficients for AP are not available, Allen *et al.* (1998) recommend $a_s = 0.25$ and $b_s = 0.50$. On the other hand, Glover and McCulloch (1958) argue that $a_s = 0.29 \cos(\phi)$ - where ϕ is the latitude - and $b_s = 0.52$ can provide reliable estimations of solar irradiance for a wide range of locations. We have not found studies aiming to calibrate or even to validate such widely used coefficients and equations for many places in northeastern Pará. Some studies (Carvalho *et al.*, 2011; Medeiros; Silva; Bezerra, 2017; Silva, 2014) that have been carried out for another locations in Brazil have shown that the calibrated coefficients for AP are usually different from the coefficients recommended by Allen *et al.* (1998) and by Glover and McCulloch (1958).

Solar radiation has a strong influence on evapotranspiration calculated by Penman-Monteith FAO 56 formula (Allen *et al.*, 1998), as Carvalho *et al.* (2011) have shown. Evapotranspiration is a major component of water balance in most locations, and as such, estimates of this variable are widely used in irrigation, crop modelling, climate risk assessment and so on. Therefore, when measurements of incoming solar radiation are not available, they must be estimated as accurately as possible. In this work, coefficients a_s and b_s of AP were fitted for six locations in northeastern Pará. Fitted coefficients are compared to the coefficients recommended by Allen *et al.* (1998) and by Glover and McCulloch (1958). A modified version of Hargreaves' formula (MH), which includes an intercept, was also calibrated. We aim to answer whether: (I) calibrated coefficients for AP differ from the coefficients recommend by both Allen *et al.* (1998) and by Glover and McCulloch (1958); (II) the use of calibrated coefficients for dry and wet season improves the performance of AP or MH for daily estimates of solar irradiance, and (III) AP and MH can properly estimate monthly average solar irradiance.

2. Material and Methods

2.1. Weather data

We used weather data recorded from 12 weather stations that belong to the Brazilian National Institute of Meteorology (INMET). The weather data comprises six locations (Fig. 1 and Table 1): Belém (BEL), Cametá (CAM), Conceição do Araguaia (CON), Marabá (MAR), Soure (SOU), and Tucuruí (TUC). There is one synoptic weather station (SWS) and one automated weather station (AWS) in each municipality listed above.

Hourly incoming solar radiation as well as maximum and minimum daily temperature were obtained from

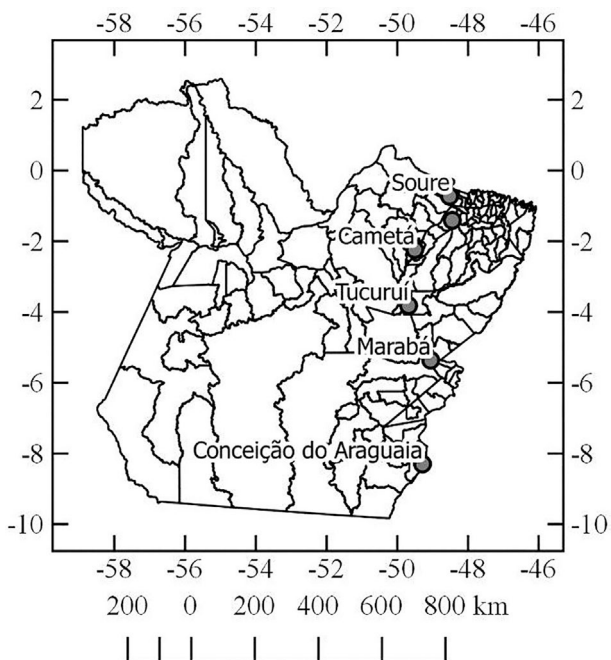


Figure 1 - Location of the weather stations used in this work.

Table 1 - Latitude, longitude, period with weather data in both AWS and SWS and duration of the dry season in each location.

Location	Latitude	Longitude	Period	Dry season
BEL	-1.4112	-48.4395	From 01-20-2003 to 12-31-2016	Aug-Nov
CAM	-2.2397	-49.4998	From 06-22-2008 to 12-31-2016	Aug-Nov
CON	-8.3036	-49.2828	From 09-04-2008 to 12-31-2016	May-Sep
MAR	-5.3664	-49.0512	From 06-25-2009 to 12-31-2016	May-Oct
SOU	-0.7278	-48.5158	From 04-27-2008 to 12-31-2016	Aug-Dec
TUC	-3.8228	-49.6750	From 03-01-2008 to 12-31-2016	Jun-Nov

each AWS. Total daily R_s was obtained from the sum of the recorded hourly R_s from 9:00 h to 21:00 h UTC, which corresponds to daytime in such locations. Days with missing records in one or more hours during daytime were disregarded. Daily records for sunshine hours (n) were obtained from the SWS in each location.

2.2. Calibrated equations

Two mathematical models aimed to estimate solar radiation were calibrated: (I) the Angström-Prescott equation (Eq. (1)), which requires daily sunshine duration hours, and (II) the Hargreaves' equation, which requires the difference between daily maximum and minimum air temperatures (ΔT) (Eq. (2)).

$$\frac{R_s}{R_a} = a_s + b_s \frac{n}{N} \quad (1)$$

$$\frac{R_s}{R_a} = a_h + b_h \sqrt{T_{max} - T_{min}} \quad (2)$$

where R_s - solar irradiance (MJ m^{-2}), R_a - extraterrestrial solar irradiance (MJ m^{-2}); n - sunshine duration hours (h); N - potential sunshine duration hours or actual day length (h); T_{max} - maximum daily air temperature ($^{\circ}\text{C}$); T_{min} - minimum daily air temperature ($^{\circ}\text{C}$); a_s , b_s , a_h , and b_h - coefficients.

Both equations were calibrated for estimates of total daily and total monthly solar irradiance. For estimates of daily solar irradiance, we also tested the calibration of seasonal (i.e., dry season and wet season) coefficients for Angström-Prescott equation (S-AP), and seasonal coefficients for modified Hargreaves' radiation formula (S-MH). The dry season was defined as the months when the potential evapotranspiration is greater than the total precipitation (Pereira, 2005), respecting the regional pattern established by Amanajás and Braga (2013), who defined the three driest months as well as the transition months between the dry and the wet season in the studied region.

Additionally, the Angström-Prescott equation as well as the Hargreaves equation were calibrated using data from all locations together, so to obtain a general equation valid for the whole region. They are abbreviated as R-AP and R-MH, respectively.

Coefficients recommended by Allen *et al.* (1998), $a_s = 0.25$ and $b_s = 0.50$ (AP-FAO), and by Glover *et al.* (1958), $a_s = 0.29 \cos(\phi)$ and $b_s = 0.52$ (AP-LAT), are also tested against the calibrated equations.

2.3. Calculations of extraterrestrial radiation and day length duration

Extraterrestrial radiation (Eq. (3)) was calculated for each day with records of both solar irradiance and sunshine duration hours according to Allen *et al.* (1998):

$$R_a = \frac{118.08}{\pi} dr [\omega_s \sin(\phi) \sin(\delta) + \cos(\phi) \cos(\delta) \sin(\omega_s)] \quad (3)$$

where dr - relative distance Earth-Sun (Eq. (4)), δ - solar declination (Eq. (5)), ω_s - hour angle at sunrise (Eq. (6)), and ϕ - latitude (radians).

$$dr = 1 + 0.033 \cos\left(\frac{2\pi}{365} j\right) \quad (4)$$

$$\delta = 0.409 \sin\left(\frac{2\pi}{365} j - 1.39\right) \quad (5)$$

$$\omega_s = \arccos[-\tan(\phi) \tan(\delta)] \quad (6)$$

$$N = \frac{\pi}{24} \omega_s \quad (7)$$

where j - day of year, N - potential sunshine duration hours or actual daylength. Based on such calculated variables and on the recorded weather data, relative incoming radiation (R_s/R_a) and relative sunshine duration (n/N) were then calculated.

Monthly averages of R_s were obtained from the average of each day that has a complete set of records. Since the weather data from AWS usually have some small gaps, a tolerance of 20% of days with missing data was adopted for computations of monthly averages of R_s . Therefore, months with less than 80% of days with a full set of records of R_s were excluded from the analysis. The average monthly R_a was calculated as the average of total daily R_a from Eq. (3), excluding from the sum all days with missing records of R_s . The same procedure and 20% tolerance were adopted for n and N .

2.4. Validation of results and statistical analysis

The performance of each model was assessed by means of the following statistical indicators: Pearson correlation coefficient (r) (Eq. (8)); Willmott's index of agreement (d) (Willmott, 1981) (Eq. (9)), which indicates how well model-produced estimates simulate observed data (Pereira *et al.*, 2018); performance index of Camargo and Sentelhas (1997) (c) (Eq. (10)), which is the result of multiplying r and d , therefore, aggregates the information provided by both indicators, making it easier to visualize; mean error (me) (Eq. (11)), which is used here to compare different models in the analysis of variance; root of mean square errors ($rmse$) (Eq. (12)), which indicates how far estimates are from their respective observed data, on average; and percent bias error ($pbias$) (Eq. (13)), which indicates the overall tendency of a model to underestimate (negative sign) or overestimate (positive sign) a variable in relation to observed data. All equation fitting, compar-

isons and analysis were performed in R.

$$r = \frac{\text{cov}(O, P)}{\sqrt{\text{var}(O)\text{var}(P)}} \tag{8}$$

$$d = 1 - \frac{\sum (O_i - P_i)^2}{\sum (|P_i - \bar{O}| + |O_i - \bar{O}|)} \tag{9}$$

$$c = rd \tag{10}$$

$$me = \frac{1}{N} \sum_{i=1}^n (P_i - O_i) \tag{11}$$

$$rmse = \sqrt{\frac{1}{N} \sum_{i=1}^N (P_i - O_i)^2} \tag{12}$$

$$pbias = 100 \frac{\sum_{i=1}^N (P_i - O_i)}{\sum_{i=1}^N O_i} \tag{13}$$

where P_i is the predicted value in the day or month i ; O_i is the observed value in the day or month i ; P is the average of predicted values; \bar{O} is the average of observed values; N is the number of samples (i.e., days or months with the necessary recorded weather data).

The calibration was performed with 70% of the available records and the validation of calibrated equation was performed with the remaining 30% of records (Table 2 and Table 3), which were chosen randomly.

Table 3 - Number of months used for calibration and validation of AP and MH for estimates of monthly solar irradiance.

Location	AP			MH		
	Calibration	Validation	Total	Calibration	Validation	Total
BEL	64	28	92	64	27	91
CAM	59	26	85	58	25	83
CON	54	23	77	57	25	82
MAR	46	20	66	53	23	76
SOU	62	26	88	66	28	94
TUC	62	27	89	71	30	101

3. Results and Discussion

3.1. Estimates of solar irradiance for daily time steps

Table 4 shows the calibrated coefficients for AP and MH. Regression analysis performed with calibration data shows significance at 1% levels for AP and MH for all locations, except for Soure, where MH is not significant. Regarding the calibrated coefficients for AP, it may be noted that, except for the intercepts of CAM and TUC, all calibrated coefficients differ from the ones recommended by Allen *et al.* (1998) and by Glover *et al.* (1958) at 1% level, which reinforces the need for calibration. Such observations are also valid for the coefficients of the Angström-Preseott equation calibrated for all locations (R-AP).

Even though the calibrated Angström-Preseott equation has a low coefficient of determination (Table 5) in some locations, such as Belém and Tucuruí, such values are usually found in other works aiming to calibrate AP, for example, in Seropédica, RJ, the coefficient of determination $r^2 = 0.83$ was found (Carvalho *et al.*, 2011), and in

Table 2 - Number of days used for calibration and validation of AP and MH for daily estimates of solar irradiance.

Location	Season	AP			MH		
		Calibration	Validation	Total	Calibration	Validation	Total
BEL	Wet	1339	540	1879	1287	576	1863
	Dry	672	324	996	697	291	988
CAM	Wet	1145	459	1604	1139	476	1615
	Dry	688	298	986	663	276	939
CON	Wet	1020	416	1436	1038	435	1473
	Dry	738	321	1059	806	371	1177
MAR	Wet	710	289	999	771	324	1095
	Dry	771	340	1111	935	397	1332
SOU	Wet	1185	518	1703	1155	489	1644
	Dry	768	344	1112	844	370	1214
TUC	Wet	1006	451	1457	1101	474	1575
	Dry	970	419	1389	1081	457	1538
Total	-	11012	4719	15731	11516	4937	16753

Table 4 - Coefficients for AP and MH and their respective confidence interval ($p \leq 0.01$). ** coefficient is significant at 1% level.

Location	Angström-Prescott			Modified Hargreaves' equation	
	a_s	b_s	$a_s + b_s$	a_h	b_h
BEL	0.227** \pm 0.009	0.352** \pm 0.015	0.579	-0.308** \pm 0.060	0.244** \pm 0.020
CAM	0.290** \pm 0.008	0.434** \pm 0.013	0.720	-0.199** \pm 0.069	0.268** \pm 0.024
CON	0.258** \pm 0.008	0.455** \pm 0.012	0.712	-0.176** \pm 0.032	0.202** \pm 0.009
MAR	0.305** \pm 0.008	0.390** \pm 0.014	0.695	-0.198** \pm 0.035	0.229** \pm 0.011
SOU	0.329** \pm 0.007	0.385** \pm 0.012	0.716	0.517** \pm 0.069	0.015 \pm 0.029
TUC	0.284** \pm 0.008	0.363** \pm 0.014	0.643	-0.088** \pm 0.047	0.200** \pm 0.017
For all locations	0.276** \pm 0.004	0.407** \pm 0.007	0.682	0.270** \pm 0.018	0.081** \pm 0.006

Table 5 - Coefficient of determination (r^2) for AP and MH obtained from calibration data for daily estimates of solar radiation.

City	Season	AP	MH
BEL	Wet	0.658	0.336
	Dry	0.463	0.107
	-	0.652	0.334
CAM	Wet	0.822	0.389
	Dry	0.707	0.088
	-	0.812	0.311
CON	Wet	0.807	0.628
	Dry	0.800	0.427
	-	0.840	0.641
MAR	Wet	0.713	0.641
	Dry	0.735	0.489
	-	0.781	0.625
SOU	Wet	0.766	0.051
	Dry	0.750	0.022
	-	0.788	0.001
TUC	Wet	0.664	0.393
	Dry	0.661	0.135
	-	0.689	0.305
For all locations	-	0.693	0.098

Parnaíba, PI, the values are $r^2 = 0.714$ and $r^2 = 0.515$, during the wet season and the dry season, respectively (Andrade Júnior *et al.*, 2012). One factor that may contribute to such large variability is the distribution of solar irradiance throughout the day. During noon, irradiance is typically greater than 970 W m^{-2} , while near the sunrise or sunset, the irradiance is usually smaller than 270 W m^{-2} , therefore, days in which the incidence of solar radiation concentrates around noon must have higher total irradiance than days in which the incidence of solar radiation concentrates near the sunrise or sunset, even if both days have the same sunshine duration hours.

Ambas and Baltas (2014) performed a spectral analysis of solar radiation in hourly time-steps in western

Macedonia and they observed that the clearness index (R_s/R_a), is about 18% higher around noon, therefore, precise estimates of solar irradiance from sunshine duration hours must consider the distribution of the periods with incidence of direct radiation throughout the day. Unfortunately, this is not a widely available information.

Table 6 shows the calibrated coefficients for S-AP and S-MH. Both S-AP and S-MH and their respective slopes are significant at 1% level in Soure, while MH is not. This indicates a strong seasonal variation of the dependence between daily total radiation and $\sqrt{\Delta T}$ in this location.

Confidence intervals for intercept and slope are also usually higher during the dry season, which may happen due to a smaller number of samples (days) (see Table 2) during the dry season. Since it is a rainy region, the dry season is shorter than the wet season.

Silva Dornelas; Silva; Oliveira (2006) observed higher standard deviations of intercept and slope of AP during the dry season in Brasília - DF, which they attributed to increased dust and biomass burning. This could possibly explain the variation of the confidence interval throughout the year in Table 6, in addition to the smaller number of samples during the dry season mentioned above. The variations of $a_s + b_s$ between dry and wet season (Table 6) also corroborate this hypothesis.

More expected, $a_s + b_s$ is usually higher during the wet season than during the dry season (Table 6), except for Belém and Tucuruí. The sum of both coefficients in AP and S-AP represents the maximum theoretical fraction of extraterrestrial radiation that can reach earth's surface in a clear sky day, since it is the result of AP when $n/N = 1$ (see Eq. (1)). Such difference in $a_s + b_s$ between seasons may be related to differences in atmospheric transparency throughout the year. According to Guyon *et al.* (2003), particle number in Amazonian atmosphere increases from about 400 cm^{-3} to about $4,000 \text{ cm}^{-3}$ when moving from the wet season to the dry season. These authors argue that this massive increase is due to the extensive seasonal biomass burning caused by deforestation and pasture cleaning. Increases in aerosol concentration could lead to dimin-

Table 6 - Coefficients for seasonal Angström-Prescott equation (S-AP) and seasonal modified Hargreaves equation (S-MH) and their respective confidence interval ($p \leq 0.01$) in each location and season. ** Significant at 1% level. * Significant at 5% level.

Location	Season	Seasonal Angström-Prescott equation (S-AP)			Seasonal modified Hargreaves equation (S-MH) ¹	
		a_s	b_s	$a_s + b_s$	a_h	b_h
BEL	Wet	0.232** \pm 0.010	0.340** \pm 0.018	0.572	-0.304** \pm 0.071	0.239** \pm 0.024
	Dry	0.209** \pm 0.028	0.383** \pm 0.041	0.592	-0.007 \pm 0.136	0.153** \pm 0.044
CAM	Wet	0.285** \pm 0.010	0.449** \pm 0.016	0.734	-0.353** \pm 0.086	0.318** \pm 0.030
	Dry	0.295** \pm 0.020	0.418** \pm 0.027	0.713	0.284** \pm 0.101	0.109** \pm 0.035
CON	Wet	0.247** \pm 0.010	0.496** \pm 0.020	0.743	-0.349** \pm 0.051	0.258** \pm 0.016
	Dry	0.243** \pm 0.017	0.460** \pm 0.022	0.703	0.026 \pm 0.061	0.149** \pm 0.016
MAR	Wet	0.297** \pm 0.012	0.407** \pm 0.025	0.704	-0.430** \pm 0.062	0.310** \pm 0.022
	Dry	0.323** \pm 0.014	0.364** \pm 0.020	0.687	-0.045* \pm 0.054	0.183** \pm 0.016
SOU	Wet	0.324** \pm 0.009	0.415** \pm 0.017	0.739	0.205** \pm 0.100	0.128** \pm 0.041
	Dry	0.325** \pm 0.015	0.374** \pm 0.020	0.699	0.714** \pm 0.065	-0.049** \pm 0.029
TUC	Wet	0.288** \pm 0.010	0.360** \pm 0.021	0.648	-0.231** \pm 0.066	0.248** \pm 0.024
	Dry	0.269** \pm 0.015	0.381** \pm 0.023	0.650	0.138** \pm 0.074	0.127** \pm 0.025

ished atmosphere transparency during the dry season, and, therefore, smaller $a_s + b_s$. Another factor contributing for higher atmospheric transparency during the wet season is aerosol scavenging, which may happen by different processes, such as nucleation scavenging and impaction scavenging (in-cloud and below-cloud). According to Ohata *et al.* (2016), nucleation scavenging controls the removal efficiency of accumulation-mode aerosols. Similar patterns of $a_s + b_s$ (higher during the wet season and smaller during the dry season) and for the confidence intervals of a_s and b_s (higher during the dry season and smaller during the wet season) are also found for another locations, such as Natal (RN) (Medeiros *et al.*, 2017) - where $a_s + b_s$ is usually greater than 0.7 during the wet season and smaller than 0.7 during the dry season - and Seropédica (RJ) (Carvalho *et al.*, 2011) - where $a_s + b_s$ averages 0.75 during summer (wet season) and 0.71 during winter (dry season).

Table 7 shows the various statistical indicator obtained by the comparison of estimated and measured R_s with validation data. AP-LAT has always the highest percent bias error and mean error, which indicates a strong tendency of this model to overestimate R_s . This tendency is also observed for AP-FAO in some locations, such as BEL, CON, and TUC, even though to a lesser extent. The poor performance of MH is demonstrated by the low Willmott's index of agreement (d) (Willmott, 1981) and the index of performance of Camargo *et al.* (1997) (c). In Soure, even though S-MH has a poor performance compared to AP or S-AP, the increase of performance when using S-MH instead of MH is remarkable.

Since MH is not significant in Soure, any $\sqrt{\Delta T}$ will result approximately the same R_s/R_a , therefore, all the var-

iation in R_s estimated by MH (in Soure) is due to variations in R_a throughout the year. This explains the extremely low performance of MH in Soure. The above-mentioned tendency of AP-LAT to overestimate R_a is clearly seen in Fig. 2. It shows that AP-LAT resulted in estimated R_s around 25 MJ m⁻² day⁻¹ when the measured R_s is around 20 MJ m⁻² day⁻¹ in Belém, which represents almost 25% overestimation.

The AP equation calibrated for the whole region (R-AP) performs similarly to AP-FAO and AP-LAT, in the sense that it tends to overestimate R_s in Belém. Also, the comparison of residual means shows that residuals of R-AP are usually different from the residuals of AP in each location. The MH equation calibrated for the whole region (R-MH) has a very poor performance, as shown by the low r , d and c , thus it cannot produce reliable estimates of R_s at daily time steps.

3.2. Estimates of monthly averages of solar radiation

Table 8 shows the calibrated coefficients for AP and MH in each location. Regression analysis performed with calibration data shows significance for both AP and MH at 1% level for all locations, except for Soure, where only AP is significant at 1% level.

Table 9 shows that the precision of estimations by both AP and MH is much better for monthly averages of solar irradiance than for daily irradiance. Even MH, which results in very imprecise estimates for daily totals of solar irradiance, could be safely used to estimate solar radiation in some locations, such as Marabá, Conceição do Araguaia, and Cametá.

Such increase in precision in monthly estimates usually happen because the relative error of one day coun-

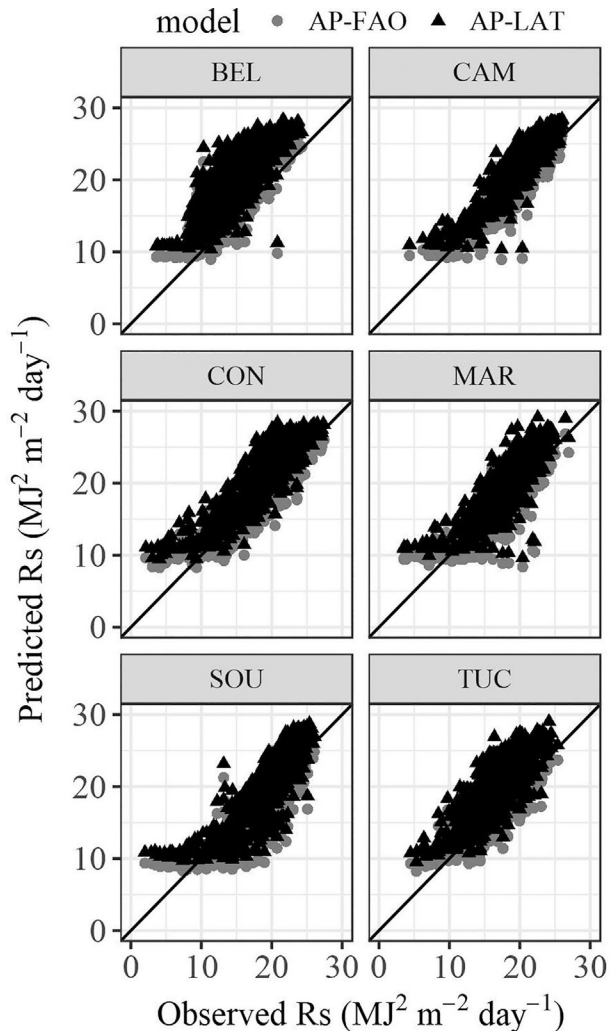


Figure 2 - Comparison between estimated R_s by AP-FAO and by AP-LAT and measured R_s for daily time steps in each location.

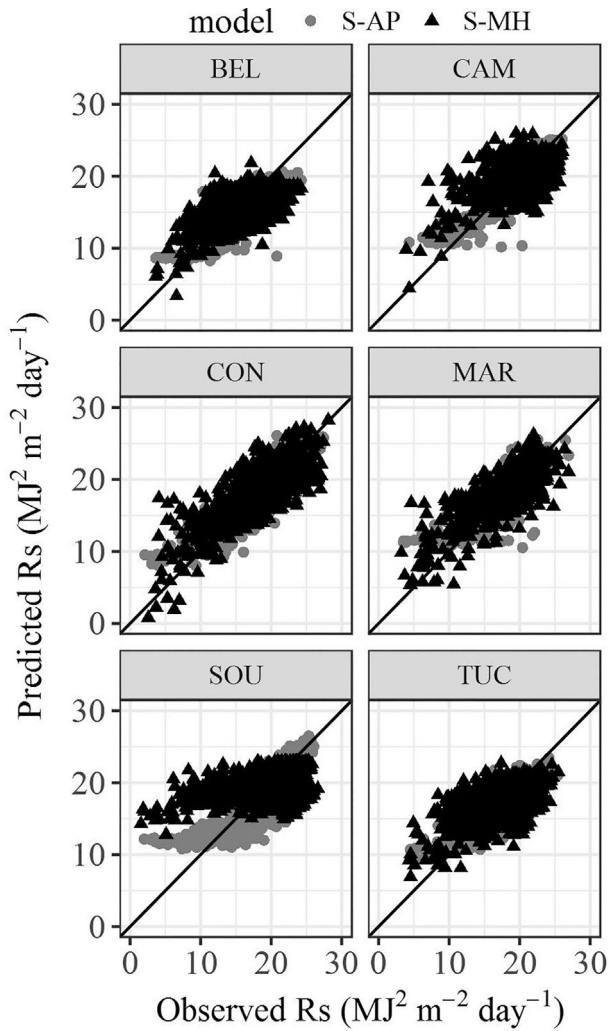


Figure 3 - Comparison between estimated R_s by S-AP and by S-MH and measured R_s for daily time steps in each location.

Table 7 - Statistical indicators of each model in each location.

Location	Model ¹		<i>r</i>	<i>d</i>	<i>c</i>	<i>me</i>	<i>rmse</i>	<i>pbias</i>
BEL	AP	a	0.796	0.877	0.698	-0.067	2.095	-0.4
	S-AP	a	0.798	0.879	0.702	-0.065	2.083	-0.4
	MH	a	0.571	0.710	0.406	0.069	2.858	0.5
	S-MH	a	0.594	0.735	0.437	0.073	2.804	0.5
	R-AP	b	0.796	0.765	0.609	2.770	3.493	18.1
	R-MH	c	0.382	0.494	0.189	3.321	4.626	21.8
	AP-FAO	c	0.794	0.718	0.570	3.714	4.412	24.2
	AP-LAT	d	0.795	0.604	0.480	5.555	6.073	36.3
CAM	AP	c	0.911	0.952	0.867	-0.036	1.490	-0.2
	S-AP	c	0.913	0.952	0.870	-0.045	1.473	-0.2
	MH	c	0.484	0.663	0.321	-0.003	3.107	0.0
	S-MH	c	0.561	0.726	0.408	0.054	2.942	0.3
	R-AP	b	0.911	0.920	0.838	-1.170	1.905	-5.7
	R-MH	a	0.331	0.475	0.157	-2.262	4.008	-11.1
	AP-FAO	c	0.911	0.953	0.869	0.047	1.570	0.2

(continued)

Table 7 - continued

Location	Model ¹		<i>r</i>	<i>d</i>	<i>c</i>	<i>me</i>	<i>rmse</i>	<i>pbias</i>
CON	AP-LAT	d	0.911	0.893	0.814	1.932	2.525	9.5
	AP	ab	0.893	0.938	0.838	-0.060	2.072	-0.3
	S-AP	b	0.899	0.944	0.849	-0.035	2.009	-0.2
	MH	ab	0.757	0.851	0.644	-0.058	2.982	-0.3
	S-MH	b	0.782	0.873	0.683	-0.033	2.852	-0.2
	R-AP	a	0.894	0.924	0.826	-0.400	2.182	-2.1
	R-MH	c	0.530	0.563	0.298	1.094	4.069	5.9
	AP-FAO	c	0.892	0.938	0.836	0.597	2.175	3.2
MAR	AP-LAT	d	0.893	0.884	0.789	2.331	3.141	12.5
	AP	b	0.850	0.913	0.776	0.049	2.097	0.3
	S-AP	b	0.853	0.915	0.780	0.062	2.082	0.3
	MH	b	0.752	0.846	0.636	0.067	2.726	0.4
	S-MH	b	0.780	0.870	0.679	0.011	2.589	0.1
	R-AP	a	0.852	0.911	0.776	-0.664	2.191	-3.6
	R-MH	b	0.479	0.499	0.239	0.456	3.701	2.5
	AP-FAO	b	0.853	0.920	0.785	0.218	2.299	1.2
SOU	AP-LAT	c	0.853	0.869	0.741	1.987	3.086	10.8
	AP	d	0.882	0.936	0.825	-0.095	2.081	-0.5
	S-AP	d	0.888	0.939	0.834	-0.084	2.026	-0.4
	MH	d	0.013	0.191	0.003	0.136	4.749	0.7
	S-MH	d	0.450	0.581	0.262	0.142	4.188	0.7
	R-AP	b	0.883	0.907	0.801	-1.577	2.621	-7.9
	R-MH	a	0.022	0.418	0.009	-3.096	5.671	-15.7
	AP-FAO	c	0.883	0.929	0.820	-0.549	2.504	-2.8
TUC	AP-LAT	e	0.883	0.911	0.805	1.302	2.874	6.5
	AP	a	0.829	0.896	0.742	0.006	2.019	0.0
	S-AP	a	0.830	0.897	0.744	0.006	2.012	0.0
	MH	a	0.541	0.705	0.382	-0.055	3.120	-0.3
	S-MH	a	0.552	0.715	0.395	-0.068	3.094	-0.4
	R-AP	b	0.826	0.898	0.742	0.522	2.111	3.1
	R-MH	b	0.380	0.512	0.194	0.857	3.506	5.0
	AP-FAO	c	0.819	0.874	0.716	1.302	2.649	7.7
	AP-LAT	d	0.821	0.777	0.638	3.091	3.891	18.3

¹Different letters indicate statistically different average of residuals.

Table 8 - Calibrated coefficients of AP and MH and their respective confidence interval ($p \leq 0.01$).

Location	Angström-Prescott			Modified Hargreaves' equation	
	a_s	b_s	$a_s + b_s$	a_h	b_h
BEL	0.234** ± 0.034	0.338** ± 0.059	0.572	-0.408** ± 0.356	0.278** ± 0.118
CAM	0.321** ± 0.026	0.384** ± 0.040	0.705	-0.565** ± 0.464	0.394** ± 0.161
COM	0.291** ± 0.031	0.397** ± 0.050	0.687	-0.044 ± 0.135	0.163** ± 0.038
MAR	0.298** ± 0.019	0.401** ± 0.033	0.699	-0.085 ± 0.135	0.194** ± 0.043
SOU	0.345** ± 0.015	0.360** ± 0.026	0.705	1.121** ± 0.530	-0.247** ± 0.225
TUC	0.299** ± 0.025	0.333** ± 0.048	0.632	0.292** ± 0.246	0.065 ± 0.087
For all locations	0.284** ± 0.022	0.391** ± 0.037	0.676	0.410** ± 0.075	0.034** ± 0.025

terbalances the relative error of another day, therefore resulting in smaller error at the end of a multi-day period (Allen *et al.*, 1998).

The same tendency of AP-FAO and AP-LAT to overestimate solar radiation, which was previously discussed, can be seen for monthly estimates as well (Table 9 and Fig. 4). In all the six locations, AP-LAT has the greatest mean error and the greatest absolute *pbias*, which indicates the use of this model results in

the greatest overestimations. The accuracy of the calibrated models (AP and MH) is higher than the accuracy of the non-calibrated models (AP-FAO and AP-LAT), however, the calibrated Hargreaves equation (MH) is much less precise than the calibrated Angström-Prescott equation (AP). Such difference is noticeable in Fig. 4, since the points representing comparisons of estimates and observed data have much higher dispersion in MH than in AP.

Table 9 - Pearson correlation coefficient (*r*), Willmott's index of agreement (*d*), performance index (*c*) of Camargo *et al.* (1995), mean error (*me*), root of mean square error (*rmse*), and percent bias error (*pbias*).

Location	Model		<i>r</i>	<i>d</i>	<i>c</i>	<i>me</i>	<i>rmse</i>	<i>pbias</i>
BEL	AP	a	0.848	0.909	0.771	-0.081	1.106	-0.5
	MH	a	0.506	0.651	0.329	0.394	1.681	2.6
	R-AP	b	0.847	0.639	0.541	2.795	3.013	18.2
	R-MH	b	0.040	0.419	0.017	3.122	3.723	20.6
	FAO	b	0.855	0.575	0.492	3.709	3.930	24.2
	LAT	c	0.853	0.456	0.389	5.558	5.722	36.3
CAM	AP	b	0.973	0.986	0.959	0.029	0.455	0.1
	MH	b	0.705	0.822	0.580	0.032	1.240	0.2
	R-AP	a	0.974	0.908	0.885	-1.126	1.211	-5.5
	R-MH	a	0.316	0.478	0.151	-2.023	2.629	-10.0
	FAO	b	0.972	0.976	0.949	0.224	0.656	1.1
	LAT	c	0.973	0.795	0.773	2.124	2.231	10.3
CON	AP	a	0.886	0.928	0.822	-0.105	0.887	-0.6
	MH	a	0.695	0.821	0.570	0.154	1.558	0.8
	R-AP	a	0.885	0.910	0.806	-0.449	0.993	-2.4
	R-MH	a	0.006	0.400	0.002	0.189	2.367	1.0
	FAO	a	0.857	0.913	0.782	0.425	1.111	2.3
	LAT	b	0.865	0.720	0.623	2.173	2.399	11.7
MAR	AP	b	0.978	0.988	0.966	0.015	0.352	0.1
	MH	ab	0.655	0.783	0.513	0.011	1.249	0.1
	R-AP	a	0.978	0.948	0.928	-0.650	0.732	-3.5
	R-MH	ab	-0.169	0.268	-0.045	-0.091	1.860	-0.5
	FAO	b	0.972	0.953	0.927	0.315	0.796	1.7
	LAT	c	0.976	0.745	0.727	2.078	2.217	11.2
SOU	AP	b	0.971	0.985	0.957	0.045	0.666	0.2
	MH	ab	0.172	0.388	0.067	-0.069	2.683	-0.3
	R-AP	a	0.974	0.916	0.892	-1.595	1.731	-8.3
	R-MH	a	-0.237	0.390	-0.092	-2.122	3.550	-10.8
	FAO	a	0.975	0.948	0.924	-0.857	1.499	-4.5
	LAT	b	0.975	0.939	0.916	0.964	1.666	5.0
TUC	AP	a	0.860	0.915	0.787	0.098	0.704	0.6
	MH	a	0.188	0.529	0.099	0.031	1.699	0.2
	R-AP	ab	0.824	0.854	0.704	0.666	1.034	3.9
	R-MH	ab	0.152	0.482	0.073	1.110	2.062	6.6
	FAO	b	0.762	0.709	0.540	1.454	1.812	8.6
	LAT	c	0.779	0.459	0.357	3.257	3.432	19.2

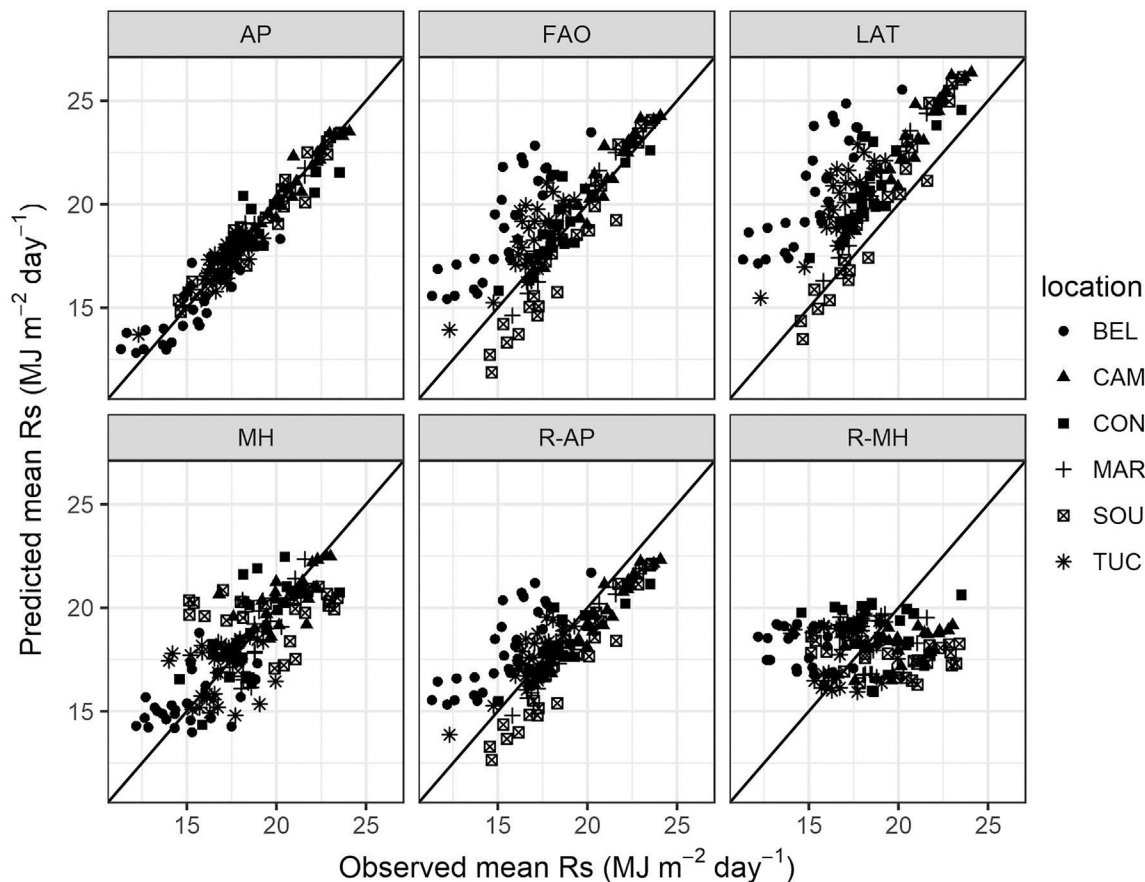


Figure 4 - Comparison between estimated and observed R_s for the six locations using monthly averages of solar radiation.

Even for monthly estimations of R_s , the MH equation calibrated for the whole region exhibits a low performance, shown by low values of r , d and c , and therefore should not be used to calculate mean R_s from mean n in any one of these locations.

4. Conclusions

1. Calibrated coefficients in the Angström-PreScott equation significantly increase the accuracy of estimates in most locations, except for Cameté. The increase in accuracy is particularly high in Belém, where the calibration reduces the percent bias error from 24.2% to -0.4%.
2. Daily estimates of solar irradiance by Hargreaves' radiation formula usually have low precision, therefore, this model is not recommended in most locations. The highest precision of MH for daily time steps occurs in Marabá, where the calibrated Hargreaves' radiation formula has $c = 0.644$, (performance index) while, on the other hand, the calibrated Angström-PreScott equation has $c = 0.838$.
3. Both the Angström-PreScott equation and the modified Hargreaves' radiation formula show a great improvement in accuracy when used to estimate monthly aver-

age solar radiation, instead of daily total solar radiation. Angström-PreScott equation is still more accurate than the modified Hargreaves' radiation formula, however Hargreaves' can be safely used to estimate monthly solar irradiance in Cameté, Conceição do Araguaia, and Marabá.

4. When calibrated coefficients for Angström-PreScott equation are not available, the use of the coefficients recommend by FAO is preferable to the ones obtained by the latitude method.

References

- ALLEN, R.G.; PEREIRA, L.S.; RAES, D.; SMITH, M. **Crop Evapotranspiration. Guidelines for computing crop water requirements**. FAO - Food and Agriculture Organization, Rome: Irrigation and Drainage Paper 56, 1998, 300 p. Available from: <http://www.fao.org/docrep/X0490E/X0490E00.htm>. Access on: 30 October 2018.
- AMBAS, V.; BALTAS, E. Spectral Analysis of Hourly Solar Radiation. **Environmental Processes**, v. 1, n. 3, p. 251-263, 2014. Available from: <https://doi.org/10.1007/s40710-014-0023-9>. Access on: 30 October 2018.
- ANDRADE JÚNIOR, A.S.; NOLETO, D.H.; SILVA, M.E.da; BRAGA, D.L.; BASTOS, E.A. Coeficientes da equação de Angström Prescott para Parnaíba, Piauí. **Comunicata Sci-**

- entiae*, v. 3, n. 1, p. 50-54, 2012. Available from: <https://www.comunicatascientiae.com.br/comunicata/article/view/103>. Access on: 30 October 2018.
- CAMARGO, A.P.; SENTELHAS, P.C. Avaliação do desempenho de diferentes métodos de estimativa da evapotranspiração potencial no estado de São Paulo, Brasil. **Revista Brasileira de Agrometeorologia**, v. 5, n. 1, p. 89-97, 1997.
- CARVALHO, D.F.de; SILVA, D.G.da; SOUZA, A.P.de; GOMES, D.P.; ROCHA, H.S. Coeficientes da equação de Angström-Prescott e sua influência na evapotranspiração de referência em Seropédica, RJ. **Revista Brasileira de Engenharia Agrícola e Ambiental**, v. 15, n. 8, p. 838-844, 2011. Available from: <https://doi.org/10.1590/S1415-43662011000800011>. Access on: 30 October 2018.
- GLOVER, J.; MCCULLOCH, J.S.G. The empirical relation between solar radiation and hours of bright sunshine in the high-altitude tropics. **Quarterly Journal of the Royal Meteorological Society**, v. 84, n. 359, p. 56-60, 1958. Available from: <http://doi.org/10.1002/qj.49708435907>. Access on: 30 October 2018.
- GUYON, P.; GRAHAM, B.; BECK, J.; BOUCHER, O.; GERASOPOULOS, E. et al. Physical properties and concentration of aerosol particles over the Amazon tropical forest during background and biomass burning conditions. **Atmospheric Chemistry Physics**, v. 3, n. 4, p. 951-967, 2003. Available from: <https://doi.org/10.5194/acp-3-951-2003>. Access on: 30 October 2018.
- MEDEIROS, F.J. de; SILVA, C.M.S.e; BEZERRA, B.G. Calibration of Ångström-Prescott equation to estimate daily solar radiation on Rio Grande do Norte state, Brazil. **Revista Brasileira de Meteorologia**, v. 32, n. 3, p. 409-416, 2017. Available from: <https://doi.org/10.1590/0102-77863230008>. Access on: 30 October 2018.
- OHATA, S.; MOTTEKI, N.; MORI, T.; KOIKE, M.; KONDO, Y. A key process controlling the wet removal of aerosols: new observational evidence. **Scientific Reports**, v. 6, n. 1, p. 34113, 2016. Available from: <https://doi.org/10.1038/srep34113>. Access on: 30 October 2018.
- PEREIRA, A.R. Simplificando o balanço hídrico de Thornthwaite-Mather. **Bragantia**, v. 64, n. 2, p. 311-313, 2005. Available from: <http://dx.doi.org/10.1590/S0006-87052005000200019>. Access on: 17 March 2019.
- PEREIRA, H.R.; MESCHIATTI, M.C.; PIRES, R.C.deM.; BLAIN, G.C. On the performance of three indices of agreement: an easy-to-use r-code for calculating the Willmott indices. **Bragantia**, v. 77, n. 2, p. 394-403, 2018. Available from: <https://doi.org/10.1590/1678-4499.2017054>. Access on: 06 March 2019.
- SILVA, A.O. Coeficientes de Angström-Prescott e sua influência na radiação solar e ETo no perímetro irrigado de bebedouro em Petrolina. **Brazilian Journal of Biosystems Engineering**, v. 8, n. 4, p. 333-342, 2014. Available from: <https://doi.org/10.18011/bioeng2014v8n4p333-342>. Access on: 30 October 2018.
- SILVA DORNELAS, K.D.e; SILVA, C.L.da; OLIVEIRA, C.A.daS. Coeficientes médios da equação de Angström-Prescott, radiação solar e evapotranspiração de referência em Brasília. **Pesquisa Agropecuária Brasileira**, v. 41, n. 8, p. 1213-1219, Aug. 2006. Available from: <https://doi.org/10.1590/S0100-204X2006000800001>. Access on: 30 October 2018.
- WILLMOTT, C.J. On the validation of models. **Physical Geography**, v. 2, n. 2, p. 184-194, 1981. Available from: <https://doi.org/10.1080/02723646.1981.10642213>. Access on: 30 October 2018.